PHYSICAL REVIEW B **70**, 081310(R) (2004)

Lattice thermal conductivity of superlattice structures

D. A. Broido
Department of Physics, Boston College, Chestnut Hill, Massachusetts 02467, USA

T. L. Reinecke
Naval Research Laboratory, Washington, DC 20375, USA

(Received 12 April 2004; revised manuscript received 16 June 2004; published 30 August 2004)

We give a quantitative inelastic phonon Boltzmann equation theory of thermal transport in quantum well superlattices due to anharmonic three phonon processes. The thermal conductivity is calculated as a function of the mass ratio of the constituent atoms and of the superlattice period. We show that there is a competition between the flattening of dispersions that inhibits heat flow and reduced umklapp scattering that enhances it. Both effects must be included consistently for a quantitative treatment. We apply this theory to realistic models of Si/Ge based structures.

DOI: 10.1103/PhysRevB.70.081310 PACS number(s): 63.22.+m, 63.20.Kr, 66.70.+f

The theory of the lattice thermal conductivity in bulk semiconductors and insulators was first formulated rigorously by Peierls.[1] He developed the earlier idea of Debye.[2] that the anharmonicity of the interatomic forces in solids causes scattering between vibrational waves, and he introduced the idea of "umklapp" processes[1] in which the phonon momentum in scattering processes is changed by a reciprocal lattice vector. Unlike phonon scattering by defects, impurities or boundaries, anharmonic umklapp scattering is an *intrinsic resistive process* that defines the minimum obtainable lattice thermal conductivity in crystalline materials, and usually dominates the behavior of the lattice thermal conductivity, κ, of bulk semiconductors at room temperature.[3]

The κ of micro- and nano-structures is of current scientific interest, and its understanding is important for potential applications, such as cooling of microelectronics and thermoelectrics.[4,5] Quantum well superlattices, nanowire arrays and carbon nanotubes are examples whose vibrational modes can differ markedly from the corresponding bulk materials. This provides the opportunity to tailor κ by materials fabrication techniques.

Superlattice structure modifies phonon dispersions by zone folding and mass mismatch between constituent layers, which changes κ through both (i) changes in the group velocities of phonons that carry heat and (ii) changes in the kinematics of phonon scattering. Previous theoretical work[6–8] used simplified models to show that zone-folding and mass mismatch resulted in reduced group velocities. These theories used a constant relaxation time approximation (CRTA) in which all phonon scattering processes are lumped into a single relaxation time, τ. The ratio κ_{SL}/τ was shown to be significantly reduced by changes in the group velocities, and order of magnitude decreases in it were obtained for Si/Ge superlattices.[6,7] In general, however, a simple constant relaxation time cannot represent the complex effects of superlattice structure on the anharmonic phonon scattering, and thus we do not have a reliable understanding of thermal transport in these systems.

In this paper, we develop for the first time a full inelastic phonon Boltzmann equation approach for the lattice thermal conductivity of superlattices resulting from three-phonon scattering processes. A central result is that the mass mismatch between constituent layers, which flattens the phonon dispersions in the superlattice, also reduces the phase space for umklapp scattering. This results in a striking competition between the decrease in phonon group velocities that acts to lower the thermal conductivity and the reduction in umklapp scattering that acts to raise it. Detailed calculations using full lattice dynamics show that the interplay between these two competing effects must be included for a quantitative description of the thermal conductivity of superlattices.

We consider a defect free superlattice and treat transport along the superlattice axis. The lowest-order anharmonic scattering process involves three phonons.[3] Conservation of energy and quasi-momentum require:

$$\omega_j(\mathbf{q}) \pm \omega_{j'}(\mathbf{q}') = \omega_{j''}(\mathbf{q}''), \quad \mathbf{q} \pm \mathbf{q}' = \mathbf{q}'' + \mathbf{K}, \tag{1}$$

where $\mathbf{q}, j$ and $\omega_j(\mathbf{q})$ are the phonon wave vector, branch index and energy, and $\mathbf{K}$ is a reciprocal lattice vector that is zero for normal processes and non-zero for umklapp processes. The combination $(\mathbf{q}, j)$, is represented by λ. We take a small temperature gradient, ∇T, to perturb the phonon distribution function: $n_\lambda = n^0_\lambda + n^1_\lambda$ with $n^1_\lambda = -(\partial n^0_\lambda/\partial\omega_\lambda)\Psi_\lambda$, where $\hbar\omega_\lambda$ is the phonon energy, $n^0_\lambda \equiv n^0(\omega_\lambda)$ is the equilibrium phonon distribution function, and Ψ_λ measures its deviation from equilibrium. The linearized phonon Boltzmann equation is:[3]

$$k_B T \mathbf{v}\cdot\nabla T \frac{\partial n^0_\lambda}{\partial T} = \sum_{\lambda'\lambda''}\left[W^+_{\lambda\lambda'\lambda''}(\Psi_{\lambda''} - \Psi_{\lambda'} - \Psi_\lambda) + \frac{1}{2} W^-_{\lambda\lambda'\lambda''}(\Psi_{\lambda''} + \Psi_{\lambda'} - \Psi_\lambda)\right], \tag{2}$$

where the three-phonon scattering rates are:

$$W^\pm_{\lambda\lambda'\lambda''} = \frac{\hbar\Omega}{32\pi^2}\frac{n^0_\lambda\left(n^0_{\lambda'} + \frac{1}{2} \pm \frac{1}{2}\right)(n^0_{\lambda''} + 1)}{\omega_\lambda\omega_{\lambda'}\omega_{\lambda''}}|\Phi_\pm(\lambda,\lambda',\lambda'')|^2 \times \delta(\omega_\lambda \pm \omega_{\lambda'} - \omega_{\lambda''})\,\delta(\mathbf{q} \pm \mathbf{q}' - \mathbf{q}'' - \mathbf{K}). \tag{3}$$

Ω is the volume of each superlattice unit cell, and the delta functions ensure energy and momentum conservation. The

three-phonon scattering matrix elements, $\Phi_{\pm}(\lambda,\lambda',\lambda'') = \Phi(j,-\mathbf{q},j';\mp\mathbf{q}';j',\mathbf{q}'')$ are given by:

$$\Phi(j,\mathbf{q},j';\mathbf{q}';j',\mathbf{q}'') = \sum_{\kappa}\sum_{\ell'\kappa'}\sum_{\ell''\kappa''}\sum_{\alpha\beta\gamma}\Phi_{\alpha\beta\gamma}(0\kappa,\ell'\kappa',\ell''\kappa'') \times e^{i\mathbf{q}'\cdot\mathbf{R}_{\ell'}}e^{i\mathbf{q}''\cdot\mathbf{R}_{\ell''}}\frac{e^{j}_{\alpha\kappa}(\mathbf{q})e^{j'}_{\beta\kappa'}(\mathbf{q}')e^{j''}_{\gamma\kappa''}(\mathbf{q}'')}{M_{\kappa}M_{\kappa'}M_{\kappa''}}. \quad (4)$$

Here, $\Phi_{\alpha\beta\gamma}(0\kappa,\ell'\kappa',\ell''\kappa'')$ is the third order force constant, $\mathbf{R}_{\ell}$ is a lattice vector in the ℓth unit cell, κ specifies an atom in the unit cell whose mass is M_{κ}, α,β,γ are Cartesian components, and the e's are phonon eigenvectors. For a given model for the interatomic potential, the dynamical matrix for the superlattice can be generated and diagonalized to obtain the phonon dispersions and modes, which form the scattering matrix elements and scattering rates in Eqs. (3) and (4).

The phonon Boltzmann equation is solved with an iterative procedure similar to that for bulk semiconductors.[9] We define: $\Psi_{\lambda}=\Sigma_{\alpha}F_{\lambda\alpha}\partial T/\partial x_{\alpha}$; putting it into Eq. (2) and rearranging we obtain:

$$F_{\lambda\alpha} = F^{0}_{\lambda\alpha} + \frac{1}{Q_{\lambda}}\sum_{\lambda'\lambda''}\Big\lfloor W^{+}_{\lambda\lambda'\lambda''}(F_{\lambda''\alpha}-F_{\lambda'\alpha}) + \frac{1}{2}W^{-}_{\lambda\lambda'\lambda''}(F_{\lambda''\alpha}+F_{\lambda'\alpha})\Big\rfloor, \quad (5)$$

where $Q_{\lambda}=\Sigma_{\lambda'\lambda''}\lfloor W^{+}_{\lambda\lambda'\lambda''}+\frac{1}{2}W^{-}_{\lambda\lambda'\lambda''}\rfloor$ and $F^{0}_{\lambda\alpha}=\hbar\omega_{\lambda}n_{0}(n_{0}+1)v_{\lambda\alpha}/(TQ_{\lambda})$. For mode $(j,\mathbf{q})$ and the other two phonon branches, j' and j'', there is a six-dimensional space of $\mathbf{q}'$ and $\mathbf{q}''$ that can form a scattering event. Momentum and energy conservation in Eq. (1) give four constraint equations that leave a two-dimensional surface in the superlattice Brillouin zone of allowed $\mathbf{q}'$. For each $(j,\mathbf{q},j',j'')$, we select q'_x and q'_y and determine the q'_z that satisfies the conservation equations. The resulting set $\{j,\mathbf{q};j',\mathbf{q}';j'',\mathbf{q}''\}$ is used in the summation to evaluate Q_{λ}. To initiate the iterative procedure, the second term on the right-hand side (RHS) of Eq. (5) is set to zero. Thus, $F^{0}_{\lambda\alpha}$ is the zeroth order solution of the Boltzmann equation. Plugging this into the RHS of Eq. (5) yields the first-order solution, $F^{1}_{\lambda,\alpha}$. The sequence is taken to converge when for large enough n, $F^{n+1}_{\lambda\alpha}\approx F^{n}_{\lambda\alpha}$. We typically find that $\sim$50 iterations is sufficient.

The heat current in the αth direction from a temperature gradient along β, $J_{\alpha}=\Sigma_{\beta}\kappa^{\alpha\beta}\partial T/\partial x_{\beta}$ defines the phonon thermal conductivity tensor:

$$\kappa^{\alpha\beta}_{SL} = \frac{1}{(2\pi)^3}\sum_{j}\int d\mathbf{q}C_{j}(\mathbf{q})v_{j\alpha}(\mathbf{q})v_{j\beta}(\mathbf{q})\tau_{j\beta}(\mathbf{q}), \quad (6)$$

where $C_{j}(\mathbf{q})=[(\hbar\omega_{j}(\mathbf{q}))^2/k_BT^2]n_{0j}(\mathbf{q})(n_{0j}(\mathbf{q})+1)$ is the contribution per mode $(j,\mathbf{q})$ to the specific heat per unit volume, and $\tau_{j\beta}(\mathbf{q})=TF_{j\beta}(\mathbf{q})/(\hbar\omega_{j}(\mathbf{q})\nu_{j\beta}(\mathbf{q}))$.

We wish to delineate in general the effects of superlattice structure on the thermal conductivity. The superlattice will be represented by varying periodically the atomic masses in alternating sets of N monolayers. We will compare the resulting superlattice thermal conductivities to those for a fictitious bulk material, called a "template," with a uniform mass M_t given by the geometric mean of the two masses in the superlattice.

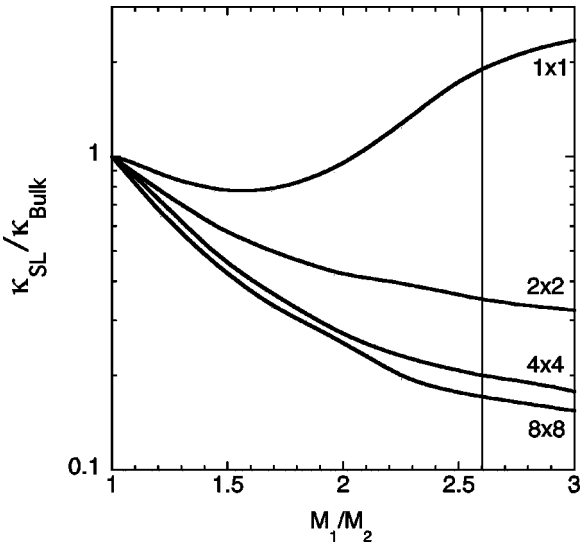

FIG. 1. Room temperature thermal conductivity of $N\times N$ superlattices along the superlattice axis, scaled by the calculated values for the bulk template (see the text), as a function of mass ratio of the constituents. The thin vertical line is for SiGe superlattices.

We take the template to have a diamond crystal structure, with atomic mass, M_t. We form an $N\times N$ superlattice made by increasing the mass of atoms in N monolayers perpendicular to the [001] direction to $M_1>M_t$ and decreasing the mass of atoms in the subsequent N monolayers to $M_2<M_t$. The $2N$ monolayer period is repeated to generate the superlattice structure. The ratio M_1/M_2 is thus increased, but we retain the geometric mean of the masses to be that of the template material: $\sqrt{M_1M_2}=M_t$.

We obtain the interatomic force constants from a Keating model,[10] which describes both bond stretching and bond bending forces in semiconductors. The second and third order contributions to the interatomic potential are parametrized by the five constants, α and β, γ, δ, and ε, chosen to fit to the second and third order elastic constants.[10]

To be definite, we take the Keating force constant parameters for the template material and the superlattices to be the geometric mean of those for Si and Ge: $\alpha_t=\sqrt{\alpha_{\mathrm{Si}}\alpha_{\mathrm{Ge}}}$, $\beta_t=\sqrt{\beta_{\mathrm{Si}}\beta_{\mathrm{Ge}}}$, etc. with $\alpha_{\mathrm{Si(Ge)}}=0.485$ (0.38), $\beta_{\mathrm{Si(Ge)}}=0.06$ (0.12), $\gamma_{\mathrm{Si(Ge)}}=-3.25$ (-2.72), $\delta_{\mathrm{Si(Ge)}}=0.25$ (0.34), and $\varepsilon_{\mathrm{Si(Ge)}}=-0.7(-0.48)$. Here, $\alpha_{\mathrm{Si(Ge)}}$ and $\beta_{\mathrm{Si(Ge)}}$ are in 10^5 dyn/cm and $\gamma_{\mathrm{Si(Ge)}}$, $\delta_{\mathrm{Si(Ge)}}$, $\varepsilon_{\mathrm{Si(Ge)}}$ are in 10^{12} dyn/cm^2.[11] Then we obtain the particular case of an Si/Ge superlattice by choosing $M_1=M_{\mathrm{Ge}}=72.6$ and $M_2=M_{\mathrm{Si}}=28.1$. The calculated thermal conductivity of the bulk template material is $\kappa_{Bulk}=0.97$ W/cm K, and we scale all superlattice results to this value. The calculated room temperature bulk thermal conductivities along [001] are 1.36 W/cm K for Si and 0.59 W/cm K for Ge, in good agreement with experiment.[12,13]

Figure 1 shows the room temperature thermal conductivity, $\kappa_{SL}/\kappa_{Bulk}$, for several superlattice periods as a function of

TABLE I. Comparison of full calculations and the constant relaxation time approximation for SiGe superlattices of the lattice thermal conductivity scaled by bulk template value (see text), $\kappa_{SL}/\kappa_{Bulk}$, and of the contributions to $\kappa_{SL}/\kappa_{Bulk}$ from the first six superlattice phonon branches. The increasing number of phonon branches with increasing period causes a decrease in the contribution per branch.

	1×1		2×2		4×4		8×8	
Branch No.	Full	CRTA	Full	CRTA	Full	CRTA	Full	CRTA
1	0.120	0.064	0.091	0.044	0.022	0.010	0.006	0.002
2	0.231	0.094	0.108	0.064	0.022	0.012	0.007	0.002
3	0.564	0.144	0.100	0.093	0.039	0.021	0.013	0.003
4	0.621	0.104	0.025	0.029	0.031	0.022	0.013	0.006
5	0.267	0.135	0.012	0.043	0.024	0.033	0.017	0.010
6	0.038	0.066	0.013	0.067	0.023	0.028	0.023	0.016
Total	1.869	0.636	0.352	0.351	0.205	0.267	0.198	0.228

M_1/M_2. For the 2×2, 4×4 and 8×8 cases, κ_{SL} decreases with increasing M_1/M_2. For fixed M_1/M_2, κ_{SL} decreases with increasing period, with nearly an order of magnitude decrease in $\kappa_{SL}/\kappa_{Bulk}$ for the 8×8 case. In all cases we find a decrease in the phase space available for umklapp scattering with increasing M_1/M_2 and with increasing period. The decreases in κ_{SL} for the 2×2, 4×4 and 8×8 cases occur because the effect of lower average group velocities along the superlattice axis outweighs the effect of decreased umklapp scattering. Then $\kappa_{SL}/\kappa_{Bulk}$ is qualitatively similar to that obtained from models using the CRTA.[6–8] When we implement the CRTA by replacing all $\tau_{j\beta}(\mathbf{q})$ in Eq. (6) with a constant, τ, we find τ-independent ratios $\kappa_{SL}/\kappa_{Bulk}$ that are in reasonably good agreement with the present full calculations for 2×2, 4×4 and 8×8 cases. This is illustrated for the specific case of Si/Ge superlattices ($M_1/M_2=2.58$) in the last row of Table I. However, this agreement is fortuitous because the contributions to $\kappa_{SL}/\kappa_{Bulk}$ from each phonon branch can differ considerably as seen in the first six rows of the table. For the 1×1 superlattice, the CRTA fails completely, as discussed below. This suggests that the good agreement between the full calculations and the CRTA obtained here for superlattices may not occur in other systems.

For fixed M_1/M_2 we find that the reduction in $\kappa_{SL}/\kappa_{Bulk}$ decreases with increasing superlattice period suggestive of the formation of a minimum. Such a behavior has been observed experimentally[14] and attributed to a change from wave-like to particle-like behavior of the phonons with increasing period.[8] The numerical complexity of our approach inhibits explicit calculations for larger period superlattices where a minimum would appear.

An interesting feature in Fig. 1 is the increase in κ_{SL} for large M_1/M_2 for the 1×1 superlattice. There is a simple physical picture to understand this. The majority of the heat is carried by the dispersive acoustic modes; the higher optic modes have low average group velocities and so carry little heat. With increasing M_1/M_2 a large gap forms between acoustic and optic modes. This reduces the scattering of the heat-carrying acoustic phonons by optic phonons. This reduced scattering overshadows the effect on κ_{SL} from the decrease in average phonon group velocity and causes the thermal conductivity to increase. Figure 2 shows the phonon dispersions for 1×1 and 2×2 SiGe superlattices ($M_1/M_2=2.58$). Note that a large gap between acoustic and optic modes occurs for the 1×1 case (solid lines) but not the 2×2 case (dashed lines). Thus, this behavior is particular to the 1×1 case.

To quantify this behavior, we define an umklapp scattering parameter, ξ as the fraction of $(j,\mathbf{q};j',\mathbf{q}')$ pairs in our search algorithm that satisfy the conservation conditions for umklapp processes ($\mathbf{K}\neq0$). ξ thus measures the phase space for three-phonon umklapp scattering processes. We also define ζ, which gives the fraction of $(j,\mathbf{q};j',\mathbf{q}')$ pairs that satisfy the conservation conditions and involve optic phonons. ξ and ζ are shown in Fig. 3 for 1×1 and 2×2 superlattices. For $M_1/M_2\geq2$, ξ and ζ decrease more for the 1×1 case than for the 2×2 case. The close correspondence between ξ and ζ shows that most umklapp processes involve at least one optic mode. The absence of the optic phonon scattering channels for the 1×1 case causes the increase in $\kappa_{SL}/\kappa_{Bulk}$ in

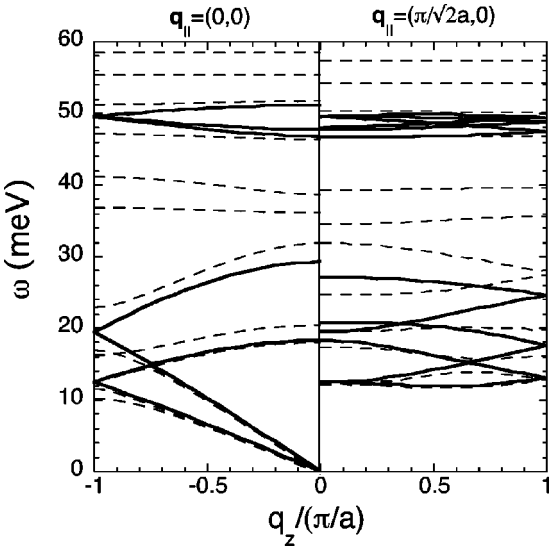

FIG. 2. Phonon dispersions along the growth direction of 1×1 (solid lines) and 2×2 (dashed lines) SiGe superlattices for two in-plane wave vectors.

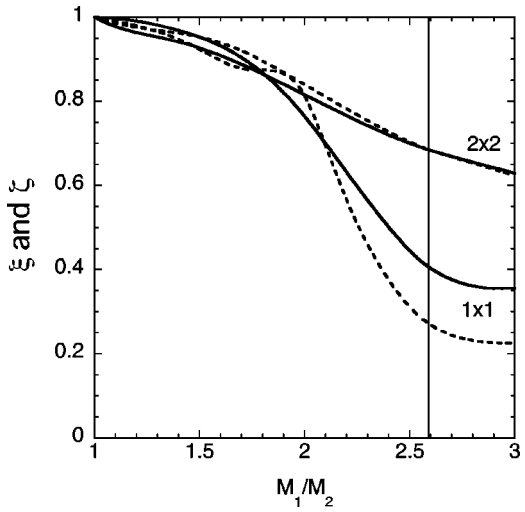

FIG. 3. Umklapp and optic phonon scattering parameters, ξ (solid lines) and ζ (dashed lines), as described in text, for 1×1 and 2×2 superlattices for increasing mass ratio of the constituents. The thin vertical line gives results for SiGe superlattices. ξ and ζ are scaled by values for the bulk template material.

Fig. 1. The CRTA fails completely for this case, predicting a decrease in $\kappa_{SL}/\kappa_{Bulk}$ in poor agreement with the full calculation (see Table I).

The qualitative features obtained here for the 1×1 superlattice have in effect already been observed. This 1×1 system is crystallographically equivalent to bulk zinc blende crystals for which experimental results are available.[15] These systems are well characterized and have limited extrinsic defects. Their thermal conductivity is controlled by intrinsic phonon scattering. The unusual behavior of the thermal conductivity of 1×1 superlattices we obtained with increasing mass ratio has been corroborated by the measurements on InSb, GaAs, InAs, GaSb, GaP, InP, and AlSb.[15] Figure 6 of Ref. 15 summarizes their results. Previous work on these systems, using a simple theoretical model, explained the initial drop-off in thermal conductivity with increasing M_1/M_2 as being due to an increase in umklapp scattering.[16] However, our results show that the umklapp scattering does not increase; rather the initial drop in κ_{SL} arises because the average phonon group velocity decreases while the umklapp scattering stays roughly constant.

We have given a rigorous treatment of anharmonic phonon scattering in superlattices. We find that the flattening of dispersions in superlattices that decreases phonon velocities also reduces the phase space for umklapp scattering. These competing effects can lead to increases as well as to decreases of κ. A unified treatment is required in order to have a quantitative measure of the κ of superlattices. Our results suggest that tailoring of the thermal conductivity in nanostructures may be possible by manipulation of phonon-phonon scattering through changes in their dispersion.

The extension of our theory to include other scattering mechanisms such as boundary and impurity scattering is straightforward and has been given for bulk semiconductors.[9] It should be noted that interface defects that occur in superlattices on the monolayer scale using current growth methods (e.g., MBE), can produce significant scattering of phonons.[17] In this case, the unusual behavior of κ_{SL} we obtain for the 1×1 superlattice could be masked.

We would like to thank G.D. Mahan and N. Mingo for stimulating and useful discussions regarding this work.

[1] R. Peierls, Ann. Phys. (Leipzig) **3**, 1055 (1929).
[2] P. Debye, *Vorträge über die Kinetische Theorie der Materie und der Elektrizität* (Teubner, Leipzig, 1914).
[3] J. M. Ziman, *Electrons and Phonons* (Cambridge University Press, Cambridge, 1960).
[4] D. G. Cahill, W. K. Ford, K. E. Goodson, G. D. Mahan, A. Majumdar, H. J. Maris, R. Merlin, and S. R. Phillpot, J. Appl. Phys. **93**, 793 (2003).
[5] R. Venkatasubramanian, E. Siivola, T. Colpitts, and B. O'Quinn, Nature (London) **413**, 597 (2001).
[6] P. Hyldgaard and G. D. Mahan, Phys. Rev. B **56**, 10 754 (1997).
[7] S. Tamura, Y. Tanaka, and H. J. Maris, Phys. Rev. B **60**, 2627 (1999).
[8] M. V. Simkin and G. D. Mahan, Phys. Rev. Lett. **84**, 927 (2000).
[9] M. Omini and A. Sparavigna, Nuovo Cimento D **19**, 1537 (1997).
[10] P. N. Keating, Phys. Rev. **145**, 637 (1966); *ibid.* **149**, 674 (1966).
[11] We find that these give a better fit to the phonon dispersions throughout the Brillouin zone and to the temperature dependent bulk thermal conductivity than those used in Ref. 10.
[12] M. G. Holland, Phys. Rev. **134**, A471 (1964).
[13] Our results are for naturally occurring Si and Ge. We have also done calculations for Keating parameters that give higher κ's corresponding to isotopically pure bulk Si and Ge [T. Ruf *et al.*, Solid State Commun. **115**, 243 (2000); M. Asen-Palmer *et al.*, Phys. Rev. B **56**, 9431 (1997)]. We find that the scaled superlattice results for that case are quantitatively similar to those given here.
[14] R. Venkatasubramanian and T. Colpitts, in *Thermoelectric Materials-New Directions and Approaches*, edited by T. M. Tritt, M. G. Kanatzidis, and H. B. Lyons, Jr., and G. D. Mahan (Materials Research Society, Pittsburgh, 1997), Vol. 478, p. 73.
[15] E. F. Steigmeier and I. Kudman, Phys. Rev. **141**, 767 (1966).
[16] M. Blackman, Philos. Mag. **19**, 989 (1935); see also Ref. 3, p. 144.
[17] S. M. Lee, D. G. Cahill, and R. Venkatasubramanian, Appl. Phys. Lett. **70**, 2957 (1997); G. Chen and M. Neagu, *ibid.* **71**, 2761 (1997).